Environ Earth Sci (2017) 76:158
DOI 10.1007/s12665-017-6478-z

ORIGINAL ARTICLE

Solidification/stabilization of tannery sludge with iron-based nanoparticles and nano-biocomposites

M. Arthy[1] · B. R. Phanikumar[2]

Received: 12 April 2016 / Accepted: 7 February 2017 / Published online: 15 February 2017

Abstract This paper presents leaching behavior of chromium from the stabilized/solidified (S/S) matrixes of tannery sludge. S/S matrixes were formed using cement, and nanoparticles and nano-biocomposites. The chromium in tannery sludge was immobilized by ZVIN (zero-valent iron nanoparticles), MIN (magnetic iron oxide nanoparticles), ZVIN–SB (zero-valent iron nanoparticles/sugarcane bagasse composite) and MIN–SB (magnetic iron oxide nanoparticles/sugarcane bagasse composite). The semi-dynamic leachate tests such as ANS 16.1 and ASTM C 1308 were performed to evaluate the efficacy of S/S matrixes. The parameters such as leaching rate, cumulative fraction leached, effective diffusivity, leachability index and leaching mechanism were calculated for the S/S matrixes containing sludge stabilized by nanoparticles and nano-biocomposites and unstabilized sludge. The leaching rate of chromium from the test specimens showed the effectiveness of nanoparticles and nano-biocomposites. Diffusion studies from the S/S matrixes indicated immobility of chromium. The mean leachability index was found to be higher than 13 for all the test specimens which shows that the S/S matrixes can be effectively utilized for 'controlled applications.' Further, nanoparticles and nano-biocomposites increased compressive strength of the S/S matrixes. XRD, SEM/EDX and FTIR revealed that chromium could be chemically fixed into cement matrixes.

Keywords Tannery sludge · Nanoparticles · Nano-biocomposites · Effective diffusivity · Leachability index

List of symbols

D_e	Effective diffusivity during leach interval (cm^2/s)
V	Volume of the specimen (cm^3)
S	Surface area of the specimen (cm^2)
T	Leaching time representing the mean time of leaching interval $T = \left[1/2\left(t_n^{1/2} + t_{n-1}^{1/2}\right)\right]^2$
a_n	Quantity of an element released from the specimen during the leaching interval (mg/L)
A_0	Total quantity of an element in the specimen at the beginning of the first leaching interval (mg/L)
Δt_n	Duration of the nth leaching interval (s)
n, m	Number of particular leaching period
b	Constant ($b = 1$ cm^2/s)
t_n	Leaching time since the beginning of the first leaching interval (s)
t_c	Cumulative time (s)
$D_{0,x}$	Diffusion coefficient of chromium in water (cm^2/s)
B_t	Cumulative flux (mg/m^2)
t	Contact time (s)
U_{max}	Maximum leachable quantity (mg/kg)
d	Bulk density of the product (kg/m^3)
B_i	Flux at time i (mg/m^2)
C	Concentration of the element released at particular time i (mg/L)

Electronic supplementary material The online version of this article (doi:10.1007/s12665-017-6478-z) contains supplementary material, which is available to authorized users.

✉ M. Arthy
ramamaruthi1288@gmail.com

B. R. Phanikumar
phanikumar_29@yahoo.com

[1] Department of Environmental and Water Resources Engineering, School of Civil and Chemical Engineering, VIT University, Vellore 632 014, India

[2] Department of Structural and Geotechnical Engineering, School of Civil and Chemical Engineering, VIT University, Vellore 632 014, India

L Volume of the extractant (L)
A Area of the specimen (m^2)

Introduction

The tanneries discharge lot of chromium-polluted water to CETP (common effluent treatment plant). CETP was considered to be an effective method for the treatment of wastewater from tanneries. In CETP, the effluents are treated at different levels. The various levels of treatment are preliminary, primary, secondary and tertiary. As an initial step in CETP, the wastewater collected from different tanneries was pretreated by passing it through screens to remove materials that can damage or clog pumps. Before pumping the wastewater to the treatment units, the quantity and quality of wastewater was maintained uniformly by mixing it in equalization tank. The wastewater was then treated chemically to remove the dissolved chromium and other chemicals by adding lime, alum and polyelectrolyte in the flash mixer. The addition of lime in the primary clarifier increases the pH of the solution which enhances the settlement of chromium due to the formation of chromium hydroxide ($Cr(OH)_3$). The wastewater is then processed biologically to remove organic and inorganic compounds. The biological treatment can be done with various treatment processes (suspended-growth processes, attached-growth processes and combined processes), but all are based on microorganisms, mainly bacteria. Microorganisms use the components of effluents as their food which breaks them down to less hazardous compounds. The sludge from the primary and secondary clarifier is then taken to sludge-drying beds for sludge dewatering. The treated water is then filtered with pressure sand and activated carbon filters to meet the standard discharge quality. However, the major environmental problem is due to the improper disposal of sludge from the primary and secondary clarifiers in landfill without any additional treatment. Cr^{3+} is the major form of chromium present in the tannery sludge. In aerobic conditions, the oxidation of Cr^{3+} to Cr^{6+} occurs if the sludge is disposed as such to the environment without any treatment. Various techniques have been developed to transform this precipitated sludge into less hazardous or non-hazardous sludge before its disposal in a landfill. One such promising technique is stabilization/solidification (S/S) of solid wastes with cementitious binders. The S/S technique has been applied to various types of waste ranging from radioactive to biological. USEPA has recognized the S/S treatment as the best technology for 57 types of waste (Shi and Spence 2004).

The solidification would not involve in chemical interaction but mechanically binds the waste and solidifying reagents (Cullinane and Jones 1986). The types of interactions that occur concurrently between the waste and solidified matrix are chemisorption, adsorption, ion exchange, precipitation, surface complexation, passivation, chemical incorporation and inclusion. In these interactions, the immobilization of waste occurs by substituting an element of similar size and charge in the cement crystal lattice. The other phenomena such as diadochy and isomorphic substitution may occur at appropriate conditions. In this phenomenon, ions of similar size with different charges from the waste can be substituted in the cement crystal structure (Yousuf et al. 1995). The S/S technique is still under development, and its chemical aspects are not yet understood clearly. Various researchers have tried to retain the hazardous waste using S/S technique (Valls and Vazquez 2002; Park and Batchelor 1999a, b; Kumpiene et al. 2008; Radovanovic et al. 2016). Shu et al. (2016) treated the electrolytic manganese residue through solidification/stabilization technique using low-grade MgO/CaO and phosphate resource. Zha et al. (2016) studied the leaching resistance of cement solidified hazardous waste after carbonation.

The binders and reagents generally used for the treatment of heavy metal-contaminated soil, sludges, slags and ashes are fly ash, cement, sulfur, lime, pH adjustment agents and phosphate (Kanchinadham et al. 2015; Phenrat et al. 2005; Wang and Vipulanandan 2000; Swarnalatha et al. 2006; Bulut et al. 2009). The chemistry of the cement, specifically in the aspect of its hydration, is a very active, challenging and controversial process. The formation of tricalcium silicate (C_3S) or alite is often used to model the hydration of the cement. The colloidal Calcium–Silicate–Hydrate gel is responsible for the strength and stability of the cement. The S/S treatment improves the stress and strain properties of the waste to facilitate their employment in construction applications, such as road or pavement subgrade, backfill, engineering fill and base material (Dermatas and Meng 2003). However, the formation of surface coating because of adding the heavy metals into the cement matrix affects the physical–chemical factors of the cement. Most of the rheological characteristics may also be affected. For example, much delay in the hydration time and reduction in compressive strength was observed in the heavy metal loaded cement matrix (Rossetti and Medici 1996). These variations in the properties of the cement must be studied before utilizing the heavy metal loaded cement matrixes in controlled applications.

In this study, the solidification/stabilization of tannery sludge by cement and cement-fly ash is presented. Before adding the tannery sludge to S/S matrixes, the immobilization of sludge was done with nanoparticles and nanobiocomposites. Nanomaterials have the potential for

incredible chemical reactivity; hence, many researchers used it for the stabilization of chromium contaminated soils or residues (Cao and Zhang 2006; Singh et al. 2011; Wang et al. 2014a, b). Generally, the addition of nanoparticles into concrete yields better workability, strength and durability of concrete (Aly et al. 2011). The detailed experimental and instrumentation analysis about the immobilization of chromium in tannery sludge by nanoparticles and nano-biocomposites was reported in our previous work (Arthy and Phanikumar 2015). This work focuses on the chromium leachability from the sludge stabilized by nanoparticles and nano-biocomposites and unstabilized sludge after incorporating it to the cement or cement/fly ash matrixes.

Objectives of this study are

1. To perform the leachability of the solidified matrixes containing unstabilized sludge and sludge stabilized with nanoparticles/nano-biocomposites using ANS 16.1 and ASTM C 1308 standards;
2. to evaluate the leaching rate, cumulative fraction leached, effective diffusivity and leachability index of the chromium from the S/S matrixes;
3. to identify the leaching mechanism of the chromium from the S/S matrixes;
4. to characterize the physical properties of the solidified matrixes; and
5. to perform the instrumentation analysis of the solidified matrixes using XRD, SEM, EDX and FTIR.

Materials and methods

Materials

Ferric chloride ($FeCl_3$), sodium dodecyl sulfate ($NaC_{12}H_{25}SO_4$), sodium hydroxide (NaOH), ammonium hydroxide solution (NH_4OH), acetic acid (CH_3COOH) and hydrochloric acid (HCl) were purchased from Sd Fine-Chem Limited. The chemical and reagents used were analytical grades. Deionized water (DIW) was used for the preparation of the stock solution. The neem leaves, sugarcane bagasse (SB) and tea waste (TW) were collected from Vellore, Tamil Nadu, India. The primary sludge was collected from CETP near Ranipet, Tamil Nadu, India. The sludge was dried in hot-air oven and stored in sealed container at 4 °C for further experimentation. The characteristics of primary sludge are shown in Table S1 (supplementary material). The binder materials used for S/S study are ordinary Portland cement (OPC) of 53 grade and Fly Ash (Class C).

Preparation of iron-based nanoparticles/nano-biocomposites

The adsorbents such as nanoparticles and nano-biocomposites have been green-synthesized using co-precipitation method. The adsorbents were then utilized for the immobilization of total chromium in tannery sludge. Figure 1 shows the schematic representation of the synthesizing procedure of nanoparticles and the nano-biocomposites. The detailed synthesizing procedure of ZVIN nanoparticles, MIN nanoparticles, ZVIN–SB nano-biocomposites and MIN–SB nano-biocomposites was reported in the previous work (Arthy and Phanikumar 2016). Briefly, the ZVIN nanoparticles were prepared by adding 0.1 N $FeCl_3$ solution drop-wise to the mixture of Solution I (tea waste extract) and SDS solution. The MIN nanoparticles were prepared by adding 16.5% of ammonia drop-wise to the mixture of Solution II (extract obtained by boiling tea waste powder in 0.2 N $FeCl_3$) and SDS solution. The MIN particles were then coated with neem leaf extract (Solution III). The ZVIN particles embedded on sugarcane bagasse nano-biocomposites (ZVIN–SB) were prepared by applying the similar procedure of ZVIN nanoparticles with a slight deviation. Appropriate quantity of sugarcane bagasse was mixed with Solution I before adding SDS and $FeCl_3$ solution. The MIN particles embedded on sugarcane bagasse nano-biocomposites (MIN–SB) were prepared by applying the similar procedure of MIN nanoparticles with a slight deviation. Appropriate quantity of sugarcane bagasse was mixed with Solution II before adding SDS, ammonia and neem leaf extract (Solution III). Sugarcane bagasse (SB) was cleaned several times with DIW and ethanol. The SB particles were dried at 80 °C in oven for 24 h and powdered. For the preparation of nano-biocomposites, the sugarcane bagasse with the particle size lesser than 150 μm was used.

Preparation of the test specimens

Test samples were prepared based on ANS 16.1 recommendations. The ANS 16.1 suggests that the L/D ratio of the specimens should be maintained within the range of 0.5–2. In this study, the PVC pipe was used for molding the materials, the L/D ratio was maintained at 1, and both the length and the diameter of the specimens were maintained at 23 mm. The volume of the PVC pipe was found to be 9.5 cm^3. In this study, 13.378 g of materials (cement/sludge/nanoparticles and nano-biocomposites) was packed in the PVC pipe of the above-specified dimensions. The composition of the different test specimens used in this study is shown in Table 1. The C/S/ZVIN, C/S/MIN, C/S/ZVIN–SB and C/S/MIN–SB represent the cement matrixes containing the sludge stabilized by nanoparticles and nano-biocomposites. The above matrixes were first subjected to

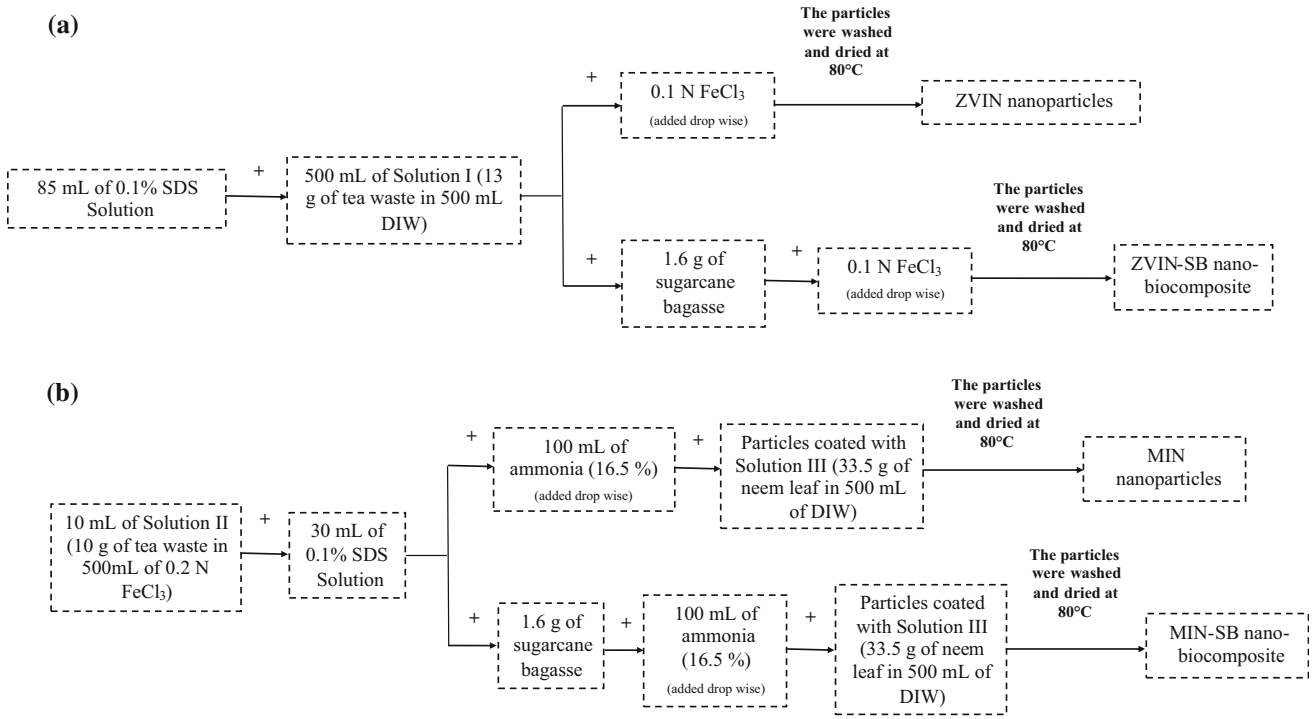

Fig. 1 Synthesizing procedure for the preparation of nanoparticles and nano-biocomposites: **a** ZVIN/ZVIN–SB and **b** MIN/MIN–SB

Table 1 Compositions of different solidified/stabilized matrixes

S/S matrix composition	Ratio	S/S matrix notations
Cement + sludge	1:1	C/S
Cement + sludge + zero-valent iron nanoparticles	1:0.9:0.1	C/S/ZVIN
Cement + sludge + magnetic iron oxide nanoparticles	1:0.9:0.1	C/S/MIN
Cement + sludge + zero-valent iron nanoparticles/sugarcane bagasse	1:0.9:0.1	C/S/ZVIN–SB
Cement + sludge + magnetic iron oxide nanoparticles/sugarcane bagasse	1:0.9:0.1	C/S/MIN–SB
Cement + fly ash + sludge	0.8:0.2:1	C/FA/S
Cement + fly ash + sludge + magnetic iron oxide nanoparticles/sugarcane bagasse	0.8:0.2:0.9:0.1	C/FA/S/MIN–SB

the leachability test in order to find the minimum chromium leachability. For optimized matrix, 20% of cement was replaced by fly ash to evaluate the leaching behavior of chromium in the cement/fly ash matrixes. C/FA/S and C/FA/S/MIN–SB represent the cement/fly ash matrixes containing unstabilized sludge and sludge stabilized by MIN–SB.

Leaching tests

This experimental program focuses on semi-dynamic leaching tests (ANS 16.1 (ANSI 1986) and ASTM C 1308 (ASTM 2008) which provide information about the release of heavy metals at 'real time' and it considers long-term leachability. They also deal with the dominant leaching mechanism from S/S wastes.

The leachants used in this study are:

1. Extractant 1 (prepared by diluting 5.7 mL of glacial acetic acid in 1 L of DIW: pH 2.88);
2. DIW (pH 6.8); and
3. Extractant 2 (prepared by diluting 5.7 mL of glacial acetic acid and 64.3 mL of 1 N NaOH, in 1 L of DIW: pH 4.93). All the experiments were performed in duplicate, and the average values are shown in graphs and tables.

ANS 16.1

According to ANS 16.1 method, experiments were conducted up to 28 days of duration (Kundu and Gupta 2008) The leachate collected during this experiment was analyzed in AAS to examine the chromium concentration. The parameters such as leaching rate (LR), cumulative fraction

leached (CFL), effective diffusivity (D_e) and leachability index (LI) can be calculated using Eqs. (1)–(4), respectively.

$$LR = \frac{a_n}{A_0}\frac{V}{St_n} \tag{1}$$

$$CFL = \frac{\sum a_n}{A_0}\frac{V}{S} \tag{2}$$

$$D_e = \pi\left[\frac{(a_n/A_0)}{\Delta t_n}\right]^2\left[\frac{V}{S}\right]^2 T \tag{3}$$

$$LI = \left(\frac{1}{m}\right)\sum_{n=1}^{m}\left(\log\left(\frac{b}{D_e}\right)\right)_n \tag{4}$$

ASTM C 1308-08

The ASTM C 1308-08 is an 11-day accelerated leach test. The diffusivity was calculated based on the assumption that the contaminant release occurs in a semi-infinite medium. Diffusivity (D_e) is calculated as

$$D_e = \frac{\pi}{t_c}\left[\frac{\sum a_n}{A_o}\frac{V}{2S}\right]^2 \tag{5}$$

Unlike ANS 16.1, the ASTM standard calculates the diffusion coefficient based on cumulative release rather than an incremental release (Mattigod et al. 2011). The LR, CFL and LI were calculated using Eqs. (1), (2) and (4).

The D_e as a function of physical retardation (τ) and chemical interaction (R) is given by Eq. (6). The $D_{o,x}$ value of Cr^{3+} in water is 5.94×10^{-6} cm^2/s (Li and Gregory 1974).

$$D_e = D_{0,x}\frac{1}{R\tau} \tag{6}$$

The leaching mechanism was determined by diffusion theory model (Groot and Sloot 1992) as given by Eq. (7).

$$\log(B_t) = \frac{1}{2}\log(t) + \log\left(U_{\max} d\sqrt{\left(\frac{D_e}{\pi}\right)}\right) \tag{7}$$

The flux and cumulative release are calculated using the following equations:

$$B_i = C \cdot \left(\frac{L}{A}\right) \tag{8}$$

$$B_t = \sum B_i \tag{9}$$

Characterization of the adsorbents and the specimens

The adsorbents such as ZVIN, MIN (iron-based nanoparticles) ZVIN–SB and MIN–SB (iron-based nano-biocomposites) were characterized with particle size analyzer, FTIR, pH_{pzc}, XRD, UV, BET, AFM, VSM, SEM and EDX. The instrumentation analysis of nanoparticles and nano-biocomposites was reported in the previous work (Arthy and Phanikumar 2016). The size of ZVIN and MIN nanoparticles was found to be 53.7 and 16.3 nm, respectively. The agglomeration of the nanoparticles was observed in AFM and SEM images. The agglomerated size of ZVIN and MIN was found to be 296.8 and 263 nm, respectively. The primary sludge from CETP was also characterized by CV, FTIR, XRD, SEM and EDX before and after the treatment process. The instrumentation analysis of primary sludge before and after the treatment process was reported in the previous work (Arthy and Phanikumar 2015).

For test specimens, the water-to-cement ratio of 0.55 was maintained for the entire study. The specimens cast in PVC molds were extracted and crushed for XRD, SEM, EDX and FTIR analysis. Further, the compressive strength, initial setting time and final setting time of the specimens were analyzed. XRD analysis was carried out with the BRUKER's D8 advance instrument using Cu Kα radiation ($\lambda = 1.54187$ Å). The surface and elemental composition of the S/S matrixes can be analyzed using scanning electron microscopy (FEI Quanta FEG 200). The SEM analysis was obtained by sprinkling the samples onto adhesive carbon tapes supported on metallic disks. The images and elemental contents of the samples were then recorded at different magnifications. The functional groups of the S/S matrixes were identified in the range of 500–4000 cm^{-1} with spectrometer (Shimadzu-IR-AFFINITY-1). The samples were mixed with KBr to make it as pellets, and they were ground in an agate mortar. The heavy metal concentration in the leachate was analyzed using Varian-AA240 atomic adsorption spectroscopy. The initial and final setting times of the specimens were determined according to ASTM C191 using Vicat needle (ASTM 2013). The unconfined compressive strength of the solidified samples after 28 days of curing was determined according to ASTM 2166 (ASTM 1991).

Results and discussion

Leaching test

The chromium in the tannery sludge was immobilized by nanoparticles and nano-biocomposites before the S/S process. The optimum conditions at which the chromium in tannery sludge was immobilized were found to be 7, 48 h and 100 g/kg, respectively, for pH, time and adsorbent dosage. At optimum conditions, the highest percentage of retention was found to be 69.9, 72, 77 and 100%,

respectively, for ZVIN, MIN, ZVIN–SB and MIN–SB (Arthy and Phanikumar 2015).

Leaching rate (LR)

Figures 2a–f and 3a–f show the leaching rate of chromium from S/S matrixes with respect to time under two different leaching tests ANS 16.1 and ASTM C 1308. The results showed that, as time increased, the leaching rate of chromium from the S/S matrixes decreased. The ANS 16.1 test shows that the leaching rate of chromium from C/S matrix with extractant 1 decreased from 1.4×10^{-9} cm/s at initial time period (2 h) to 1.07×10^{-11} cm/s at final time period (672 h) (Fig. 2a). Figure 2b shows the leaching rate of chromium from C/S matrix with extractant 1 decreased from 1.42×10^{-9} cm/s (2 h) to 9.05×10^{-12} cm/s (264 h) (ASTM C 1308). A similar decreasing trend was observed with other extractants (Fig. 2c–f) also. The S/S matrixes containing stabilized sludge with nanoparticles and nano-biocomposites have considerably reduced the leaching rate of chromium. For instance, at final time period in ANS 16.1 (672 h) and ASTM C 1308 (264 h) leach tests, the specimens C/S/ZVIN, C/S/MIN, C/S/ZVIN–SB and C/S/MIN–SB showed greater than 95% reduction in the leachability of chromium with respect to C/S matrix in all leaching solutions. In ANS 16.1 test method, with extractant 1, the leaching rate of C/FA/S matrix reduced from 2.5×10^{-9} (2 h) to 3.5×10^{-11} cm/s (672 h), whereas in ASTM C 1308 leach test, the leaching rate of chromium reduced from 1.11×10^{-9} (2 h) to 1.77×10^{-11} (264 h) (Fig. 3a, b). The similar trend was observed with other extractants (Fig. 3c–f) also. The addition of MIN–SB stabilized sludge to the cement/fly ash matrix clearly shows that the leaching rate of chromium reduced to 99.7% (ANS 16.1) and 67.8% (ASTM C 1308) with respect to C/FA/S matrix at 672 and 264 h, respectively.

Cumulative fraction leached (CFL)

The cumulative fraction of chromium leached from the S/S matrixes with various extractants under ANS 16.1 and ASTM C 1308 is shown in Figures S1 and S2 (supplementary material). The CFL value of the S/S matrixes at 672 and 264 h, respectively, for ANS 16.1 and ASTM C 1308 leach tests is given in Table 2. The results show that the sludge stabilized with nanoparticles and nano-biocomposites has shown less cumulative chromium concentration in the leachate when compared with unstabilized sludge. The mobility of chromium ions in the leachants was found to be of the following order DIW < extractant 2 < extractant 1.

Effective diffusivity (D_e)

The mean effective diffusivity (D_e) of the S/S matrixes is given in Table 3. The S/S matrix with unstabilized sludge resulted in higher diffusivity of chromium in all leaching solutions. Therefore, the mobility of chromium from the S/S matrix decreased when the sludge was treated with nanoparticles (ZVIN, MIN) and nano-biocomposites (ZVIN–SB and MIN–SB). D_e values usually vary between 10^{-5} (very mobile) and 10^{-15} (immobile) (Nathwani and Phillips 1980). Thus, in this study, the values of D_e suggest that chromium in all the specimens was immobile. The D_e values of C/S, C/S/ZVIN, C/S/MIN, C/S/ZVIN–SB and C/S/MIN–SB matrixes were high when compared with C/FA/S and C/FA/S/MIN–SB. When DIW was used as leachant, chromium did not leach from the C/S/MIN–SB matrix. Hence, zero diffusivity was obtained (Table 3). The values of physical retardation (τ) and chemical retention (R) of all the S/S matrixes are given in Table 3. The $R\tau$ value was found to be highest (at least one order magnitude) for the sludge stabilized by nanoparticles and nano-biocomposites than for the unstabilized sludge. This may be due to the occupation of nanoparticles and nano-biocomposites in pores of the matrixes, which results either in partial wetting of the material or the pores may not be wetted at all.

Leachability index (LI)

The effectiveness of the S/S matrix can be assessed by its leachability index. This can be used as a performance criterion for the utilization of S/S matrix. If LI is above 9, the S/S matrix can be used in controlled utilization, i.e., the S/S matrixes are acceptable for quarry rehabilitation, lagoon closure, road-base material, etc. (Dermatas et al. 2004). Table 3 shows the mean LI of all the S/S matrixes was higher than 13. LI of the S/S matrixes containing sludge stabilized by nanoparticles and nano-biocomposites was found to be higher than the C/S and C/FA/S matrixes. Thus, based on protocol proposed by Environment Canada's Wastewater Technology Centre (Wastewater Technology Centre 1991), all the S/S samples were acceptable for controlled utilization.

Leaching mechanism

Figures 4a–f and 5a–f show the logarithmic representation of cumulative flux and time of S/S matrixes for ANS 16.1 and ASTM C 1308 leaching tests. The mechanism controlling the leaching of chromium from the S/S matrixes is given in Table 4. From the range of slope values, the dominant leaching mechanism can be identified as follows:

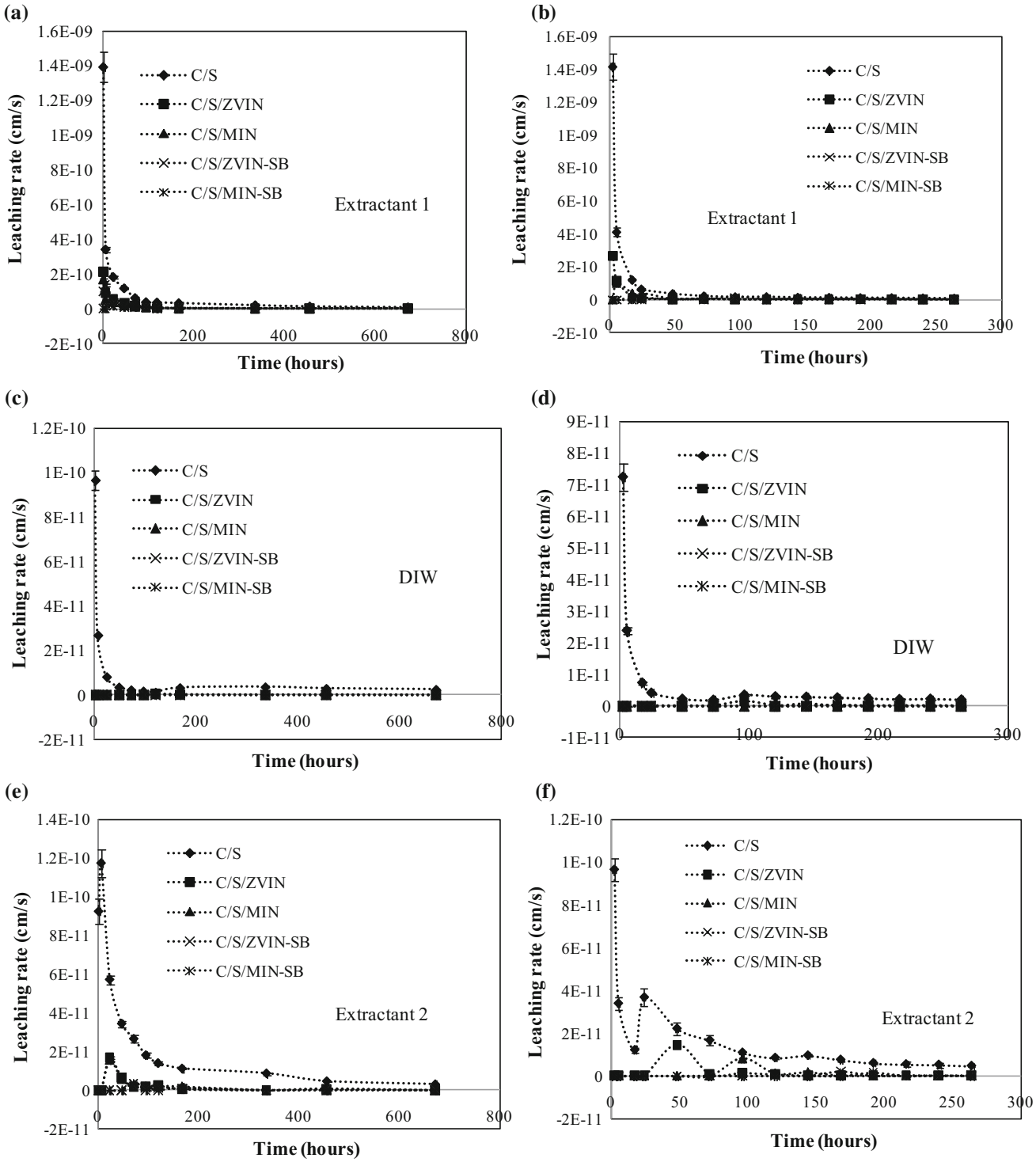

Fig. 2 Variation of leaching rate (LR) of the cement-based S/S matrixes with respect to time: ANS 16.1 (**a** extractant 1, **c** DIW and **e** extractant 2) and ASTM C 1308 (**b** extractant 1, **d** DIW and **f** extractant 2)

1. if slope = 1 (slope > 0.65): dissolution;
2. if slope is close to 0.5 (0.35 < slope ≤ 0.65): diffusion; and
3. if the slope is close to zero (slope ≤ 0.35): initial wash-off.

If the experimental points do not lie on a line, then the leaching mechanism is found to be variable with time (Sloot et al. 1989; Torras et al. 2011). Table 4 shows that, in all leachants, the S/S matrix containing sludge stabilized with nanoparticles and nano-biocomposites

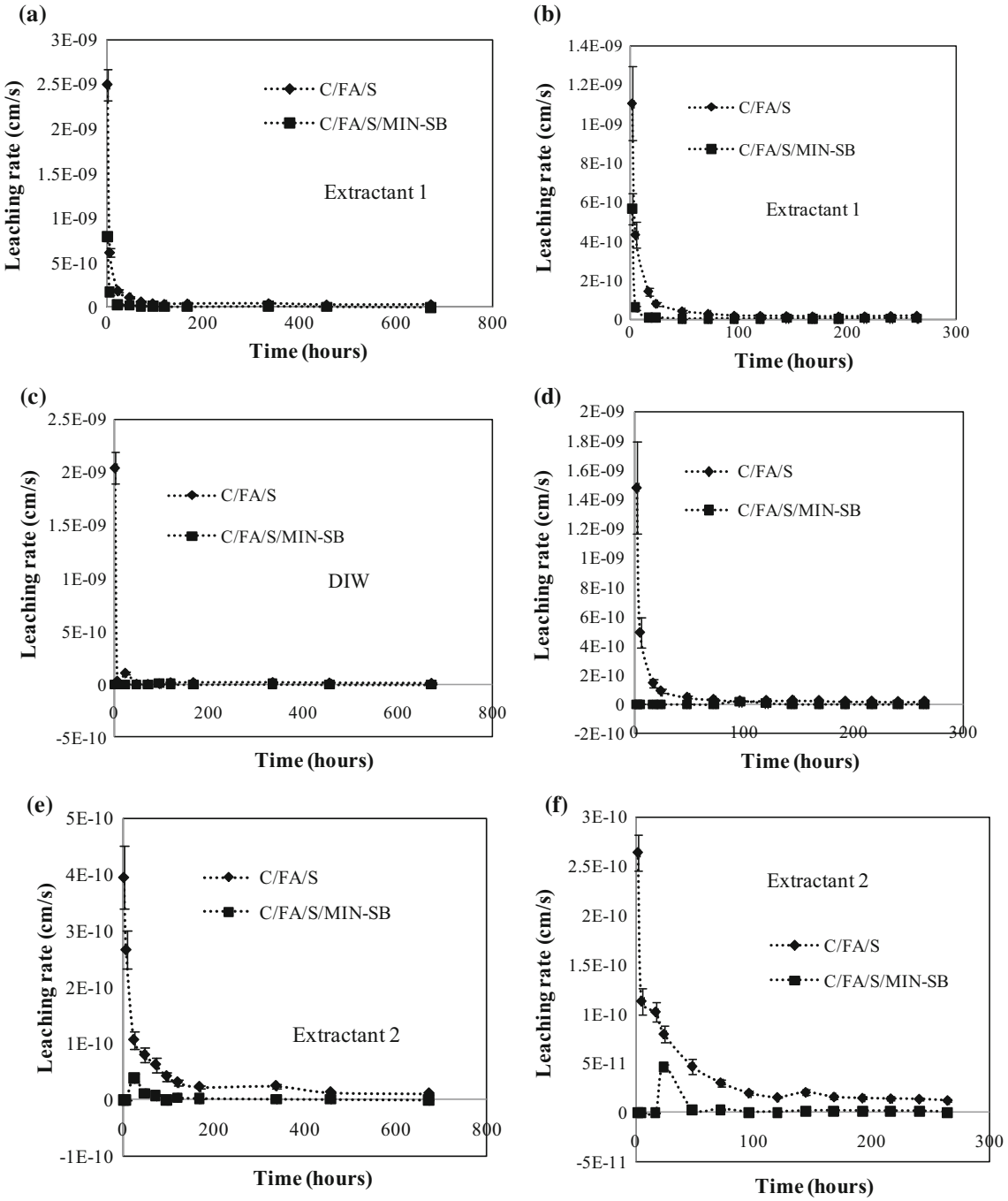

Fig. 3 Variation of leaching rate (LR) of the cement/fly ash-based S/S matrixes with respect to time: ANS 16.1 (**a** extractant 1, **c** DIW and **e** extractant 2) and ASTM C 1308 (**b** extractant 1, **d** DIW and **f** extractant 2)

indicates diffusion as the dominant leaching mechanism. This means that the release of chromium occurred through the pores of the matrixes. The C/S matrix has shown dissolution as the major leaching mechanism in all the leachants except with extractant 2 (ASTM C 1308), where the slope was found to be greater than 1. Hence, the mechanism was found to vary with respect to time. A similar result was obtained for C/S/FA matrix when DIW (ANS 16.1) and extractant 2 (ASTM 1308) were used as leachants.

Mechanism of chromium binding

The oxidation–reduction reaction is important in the immobilization of contaminants with multiple oxidation states. They have different chemical or toxicological

Table 2 Cumulative fraction of chromium leached from S/S matrixes

Matrix	ANS 16.1			ASTM C 1308		
	Extractant 1	DIW	Extractant 2	Extractant 1	DIW	Extractant 2
Cumulative fraction leached (cm)						
C/S	4.89×10^{-3}	5.62×10^{-4}	1.64×10^{-3}	3.61×10^{-3}	6.17×10^{-4}	1.79×10^{-3}
C/S/ZVIN	5.82×10^{-4}	2.7×10^{-5}	1.58×10^{-4}	5.11×10^{-4}	2.47×10^{-5}	1.46×10^{-4}
C/S/MIN	3.85×10^{-4}	1.5×10^{-5}	1.4×10^{-4}	3.46×10^{-4}	1.56×10^{-5}	1.46×10^{-4}
C/S/ZVIN–SB	3.46×10^{-4}	1.1×10^{-5}	8.37×10^{-5}	3.13×10^{-4}	1.13×10^{-5}	7.8×10^{-5}
C/S/MIN–SB	2.16×10^{-4}	0	7.0×10^{-5}	2.11×10^{-4}	0	6.6×10^{-5}
C/FA/S	8.6×10^{-3}	3.13×10^{-3}	4.23×10^{-3}	4.59×10^{-3}	6.03×10^{-3}	4.25×10^{-3}
C/FA/S/MIN–SB	1.7×10^{-3}	3.30×10^{-4}	3.90×10^{-4}	1.3×10^{-3}	3.89×10^{-4}	3.59×10^{-5}

behaviors in various redox states. For instance, Cr^{6+} is highly toxic and mobile than Cr^{3+}. The tannery sludge collected from CETP contains 96% of Cr^{3+} and 4% of Cr^{6+}. The Cr^{3+} ions on the surface of iron nanoparticles generate $Cr_xFe_{1-x}OOH$ or $(Cr_xFe_{1-x})(OH)_3$ compounds (Powell et al. 1995; Li et al. 2008). Fe^{3+} ions are replaced with Cr^{3+} and get included into iron oxy-hydroxide shell of iron, which results in the formation of Cr–Fe mixed oxides/hydroxides/oxyhydroxides ($Cr_xFe_{1-x}(OH)_3$ and $Cr_2O_3.FeO$). The replacement of Cr^{3+} and Fe^{3+} ions occurs due to their similar charge and ionic radii (Cr^{3+}—0.615 Å, Fe^{3+}—0.645 Å) (Singh et al. 2012). In most of the conditions, Cr^{3+} got more significantly sorbed or precipitated than Cr^{6+}. Equation 10 elucidates the adsorption of trivalent chromium ions on the surface of iron oxide nanoparticles. The Cr^{3+} can also be partly replaced with Fe^{3+} through ion-exchange mechanism (Eq. 11) (Wang et al. 2014a, b). Equations 12 and 13 illustrate the formation of iron–chromium precipitate.

$$Cr^{3+} + Fe_3O_4 \rightarrow Cr^{3+} \cdot Fe_3O_4 \quad (10)$$

$$2Cr^{3+} + Fe_3O_4 \rightarrow Cr_2O_3 \cdot FeO + 2Fe^{3+} \quad (11)$$

$$xCr^{3+} + (1-x)Fe^{3+} + 3H_2O \rightarrow (Cr_xFe_{1-x})(OH)_3 + 3H^+ \quad (12)$$

$$xCr^{3+} + (1-x)Fe^{3+} + 2H_2O \rightarrow Cr_xFe_{1-x}OOH + 3H^+ \quad (13)$$

The XRD results show the presence of iron chromium oxides ($FeCr_2O_4$ and $Cr_{1.3}Fe_{0.7}O_3$) in the S/S matrixes. Further, the formation of calcium chromium sulfite hydrate ($CaCr_2O_6SO_3 \cdot 11H_2O$) and calcium aluminum chromium oxide sulfate hydrate ($Ca_4Al_2Cr_{0.5}O_{10}(SO_4)_{0.5} \cdot 16H_2O$) in the S/S matrixes confirms the immobilization of chromium ions in the cement matrixes.

The possible reactions for the conversion of Cr^{6+} to Cr^{3+} in the presence of iron nanoparticles are given by the following equations.

$$3Fe^0 + 2CrO_4^{2-} + 10H^+ \rightarrow 3Fe^{2+} + 2Cr(OH)_3 + 2H_2O \quad (14)$$

$$3Fe^0 + Cr_2O_7^- + 7H_2O \rightarrow 3Fe^{2+} + 2Cr(OH)_3 + 8OH^- \quad (15)$$

The stabilization of contaminants with cement generally provides a moderately oxidizing environment, but the addition of reducing agents promotes the reduction of contaminants to enhance the immobilization (Taylor 1990; Lea 1971). Thus, the presence of iron nanoparticles and nano-biocomposites in the sludge provides the long-term reducing ability and protect Cr^{3+} from re-oxidation and subsequent leaching.

Characterization of the S/S specimen

Physical characterization

The physical characterization of the S/S matrix is shown in the supplementary material (Figure S3). The compressive strength of the S/S matrixes was found to be 0.502, 0.521, 0.542, 0.542, 0.762, 0.421 and 0.722 MPa, respectively, for C/S, C/S/ZVIN, C/S/MIN, C/S/ZVIN–SB, C/S/MIN–SB, C/FA/S and C/FA/S/MIN–SB (Figure S3 (a)). The S/S material with unconfined compressive strength of 0.35 MPa was considered to be satisfactory by EPA. This has been suggested to provide a stable foundation for materials placed upon it in a landfill (Malviya and Chaudhary 2006). In this study, strength of all the S/S matrixes was found to be above the limit specified by EPA. Specifically, the strength of a solidified matrix with MIN–SB stabilized sludge was higher than the other S/S matrixes. The initial setting time was found to be 85, 74, 73, 71, 70, 75 and 70 min, respectively, for C/S, C/S/ZVIN, C/S/MIN, C/S/ZVIN–SB, C/S/MIN–SB, C/FA/S and C/FA/S/MIN–SB matrixes (Figure S3 (b)). The final setting time was found to be 520, 495, 475, 480, 470, 480 and 465 min, respectively, for C/S, C/S/ZVIN, C/S/MIN, C/S/ZVIN–SB, C/S/MIN–SB, C/FA/S and C/FA/S/

Table 3 Diffusivity, physical retardation (τ), chemical retention (R) and leachability index of the S/S matrixes

Matrix	Extractant 1			DIW			Extractant 2		
	Diffusivity	$R\tau$	Leachability index	Diffusivity	$R\tau$	Leachability index	Diffusivity	$R\tau$	Leachability index
ANS 16.1									
C/S	1.17×10^{-13}	5.08×10^{7}	13.16	1.06×10^{-15}	5.6×10^{9}	15.48	1.51×10^{-14}	3.93×10^{8}	14.22
C/S/ZVIN	3.63×10^{-15}	1.64×10^{9}	15.08	3.16×10^{-17}	1.88×10^{11}	17.31	3.507×10^{-16}	1.69×10^{10}	16.28
C/S/MIN	1.93×10^{-15}	3.08×10^{9}	15.70	1.07×10^{-17}	5.55×10^{11}	18.11	3.51×10^{-16}	1.69×10^{10}	16.24
C/S/ZVIN–SB	1.73×10^{-15}	3.43×10^{9}	15.84	2.41×10^{-18}	2.46×10^{12}	18.56	1.33×10^{-16}	4.47×10^{10}	16.77
C/S/MIN–SB	7.65×10^{-16}	7.76×10^{9}	16.03	NIL	NIL	NIL	1.677×10^{-16}	3.54×10^{10}	16.82
C/FA/S	2.47×10^{-13}	2.4×10^{7}	12.83	3.79×10^{-14}	1.57×10^{8}	14.17	8.31×10^{-14}	7.15×10^{7}	13.41
C/FA/S/MIN–SB	1.41×10^{-14}	4.21×10^{8}	14.35	3.04×10^{-15}	1.95×10^{9}	15.18	1.22×10^{-15}	4.87×10^{9}	15.27
ASTM C 1308									
C/S	1.013×10^{-14}	5.86×10^{8}	14.02	1.48×10^{-16}	4.01×10^{10}	16.08	1.75×10^{-15}	3.39×10^{9}	15.08
C/S/ZVIN	3.19×10^{-16}	1.86×10^{10}	15.55	1.28×10^{-18}	4.64×10^{12}	17.91	3.523×10^{-17}	1.69×10^{11}	16.47
C/S/MIN	1.75×10^{-16}	3.39×10^{10}	15.78	3.94×10^{-19}	1.51×10^{13}	18.41	4.44×10^{-17}	1.34×10^{11}	16.37
C/S/ZVIN–SB	1.10×10^{-16}	5.4×10^{10}	15.98	1.93×10^{-19}	3.08×10^{13}	18.72	8.507×10^{-18}	6.98×10^{11}	17.07
C/S/MIN–SB	1.04×10^{-16}	5.71×10^{10}	16.00	NIL	NIL	NIL	6.307×10^{-18}	9.42×10^{11}	17.20
C/FA/S	1.15×10^{-14}	5.17×10^{8}	13.98	1.96×10^{-14}	3.03×10^{8}	13.77	8.54×10^{-15}	6.96×10^{8}	14.28
C/FA/S/MIN–SB	7.36×10^{-16}	8.07×10^{9}	15.31	2.21×10^{-16}	2.69×10^{10}	15.66	1.54×10^{-16}	3.86×10^{10}	15.83

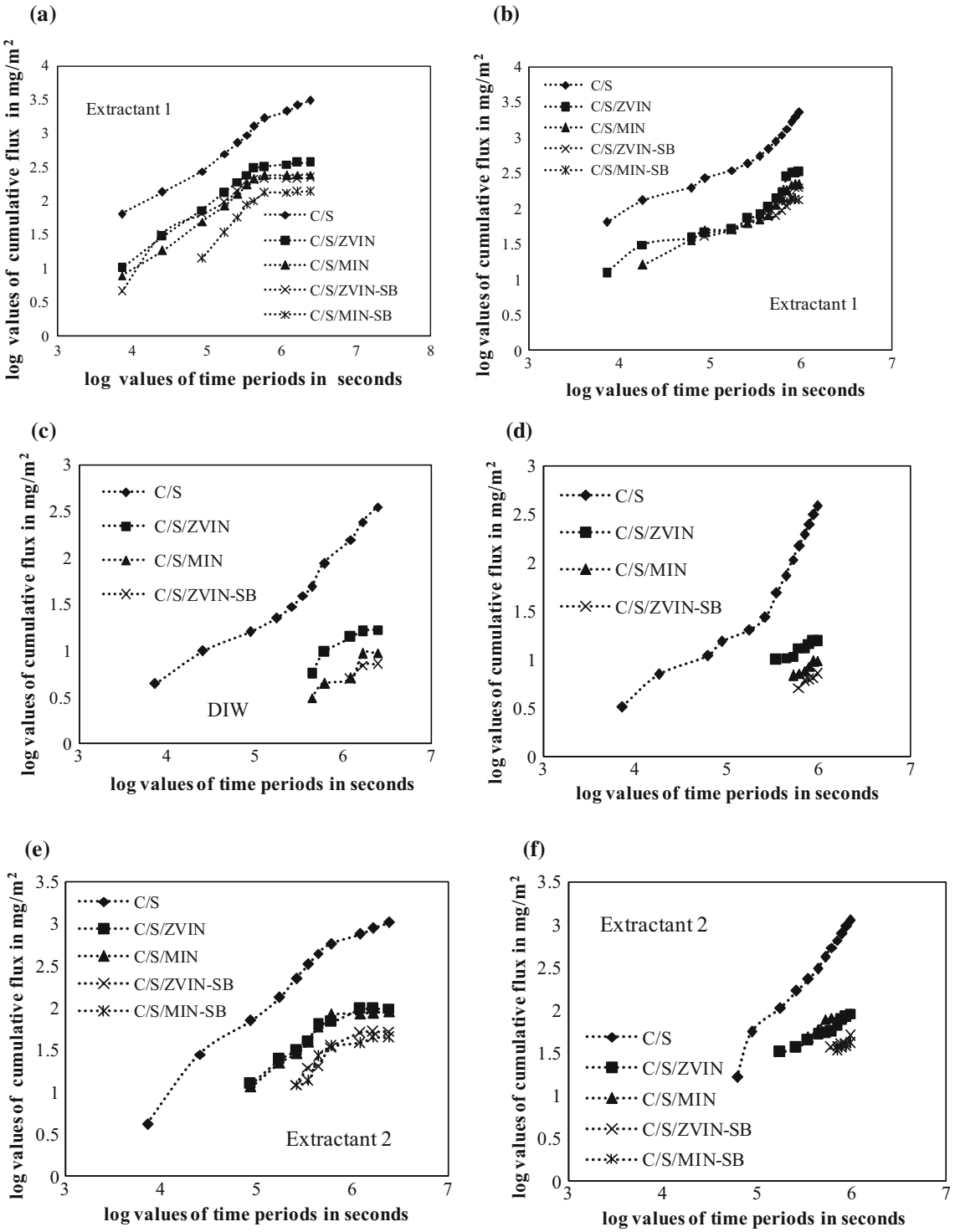

Fig. 4 Variation of cumulative flux of chromium leached from the cement-based S/S matrixes: ANS 16.1 (**a** extractant 1, **c** DIW, **e** extractant 2) and ASTM C 1308 (**b** extractant 1, **d** DIW and **f** extractant 2)

MIN–SB matrixes (Figure S3 (b)). Thus, the addition of nanoparticles and nano-biocomposites has increased the compressive strength and decreased the final setting time of the S/S matrixes when compared with C/S and C/FA/S matrixes.

Instrumental characterization

X-ray diffraction (XRD) analysis The XRD analysis of the S/S matrixes at 1st, 5th and 28th day of hydration is given in the supplementary material (Figures S4; S5; S6

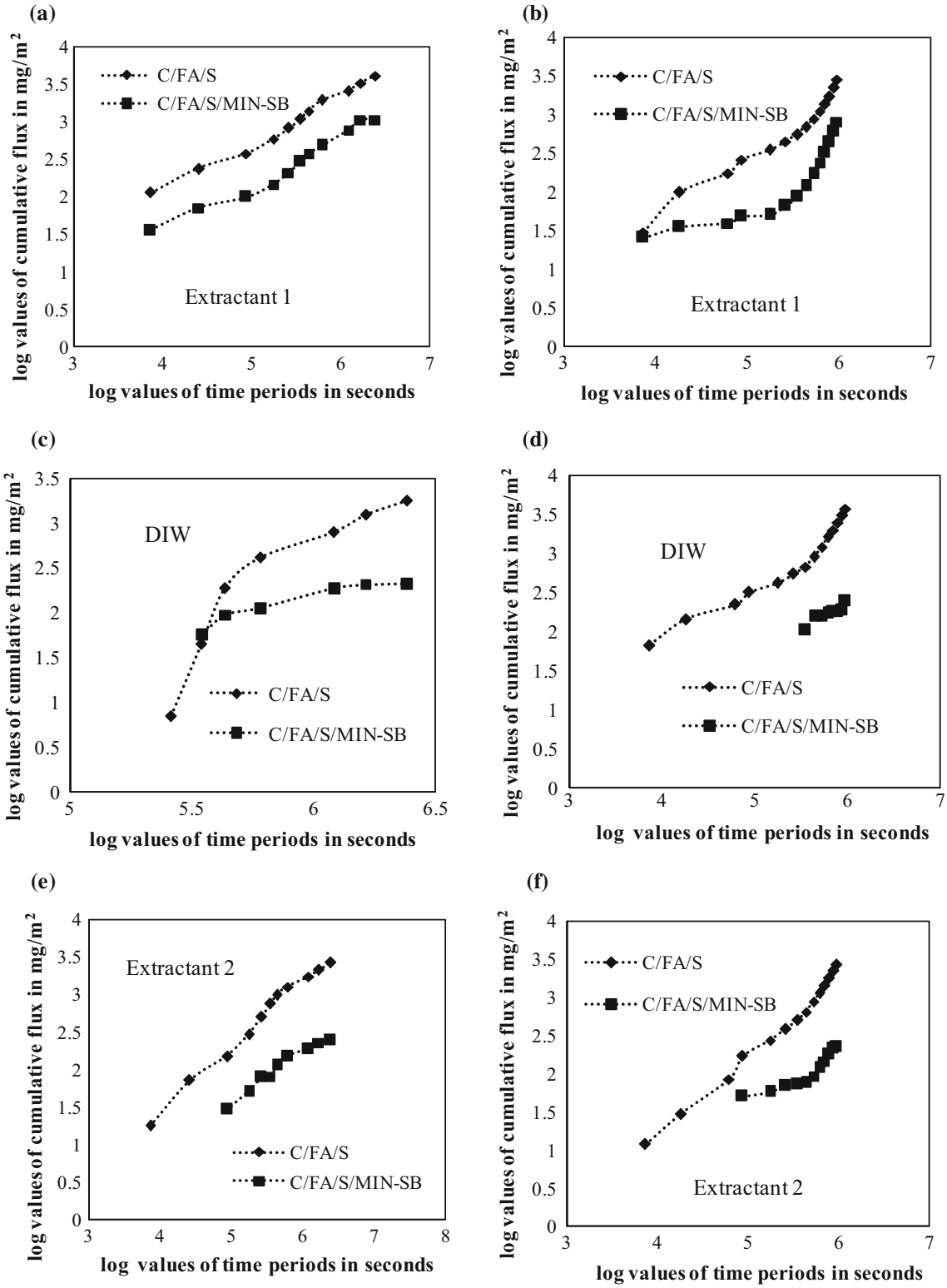

Fig. 5 Variation of cumulative flux of chromium leached from the cement/fly ash-based S/S matrixes: ANS 16.1 (**a** extractant 1, **c** DIW, **e** extractant 2) and ASTM 1308 (**b** extractant 1, **d** DIW and **f** extractant 2)

and Tables S2; S3). Chromium stabilization in cement has been investigated by several authors (Heimann et al. 1992; Mollah et al. 1992). The C–S–H has a high specific surface area with high density of irregular hydrogen bonding, which creates a strong potential for sorption. The first formed C–S–H dose has high chemical reactivity with

Table 4 Leaching mechanism of the solidified/stabilized matrixes

Matrix	Extractant 1				DIW				Extractant 2			
	ANS 16.1		ASTM 1308		ANS 16.1		ASTM 1308		ANS 16.1		ASTM 1308	
	Slope	Mechanism	Slope	Mechanism	Slope	Mechanism	Slope	Mechanism	Slope	Mechanism	Slope	Mechanism
C/S	0.706	Dissolution	0.683	Dissolution	0.747	Dissolution	0.953	Dissolution	0.942	Dissolution	1.168	Varying with time
C/S/ZVIN	0.649	Diffusion	0.629	Diffusion	0.614	Diffusion	0.503	Diffusion	0.636	Diffusion	0.618	Diffusion
C/S/MIN	0.643	Diffusion	0.645	Diffusion	0.649	Diffusion	0.642	Diffusion	0.632	Diffusion	0.606	Diffusion
C/S/ZVIN–SB	0.631	Diffusion	0.645	Diffusion	0.503	Diffusion	0.639	Diffusion	0.649	Diffusion	0.614	Diffusion
C/S/MIN–SB	0.649	Diffusion	0.505	Diffusion	NIL	NIL	NIL	NIL	0.576	Diffusion	0.632	Diffusion
C/FA/S	0.636	Diffusion	0.822	Dissolution	2.154	Varying with time	1.704	Dissolution	0.876	Dissolution	1.103	Varying with time
C/FA/S/MIN–SB	0.622	Diffusion	0.648	Diffusion	0.643	Diffusion	0.641	Diffusion	0.643	Diffusion	0.649	Diffusion

resulting sorption and inclusion of toxics (heavy metals) to cement grains. Based on the pH of the matrixes, the immobilization of toxics can be done by chemisorption, precipitation, substitution, ion exchange or adsorption on the external surface/cavities of C–S–H gel. The immobilization of chromium was done by substituting chromium for silicon and aluminum. Chromium (Cr^{3+}) increases the Ca/Si ratio in the C–S–H phases (Omotoso et al. 1995; Lee 2004). The following observations from XRD analysis confirmed the immobilization of chromium.

1. The presence of calcium chromate ($CaCrO_4$, $Ca(CrO_4)_2$ and $Ca_5(CrO_4)3O_{0.5}$), calcium chromium hydrate ($CaCrO_4{\cdot}2H_2O$ and $CaCrO_4{\cdot}H_2O$), calcium aluminum oxide chromium hydrate ($Ca_4Al_2CrO_{10}{\cdot}12H_2O$, $Ca_6Al_2Cr_3O_{18}{\cdot}32H_2O$ and $Ca_4Al_2O_6(CrO_4){\cdot}9H_2O$) in the hydrated cement/sludge matrixes indicates the substitution of chromium for silicon ions (Tables S2 and S3);
2. Many crystalline phases that form during the hydration process are amenable for substitution reaction. For instance, hydration of $Ca_3Al_2O_6$ in the presence of cement/gypsum yields ettringite ($3CaO{\cdot}Al_2O_3{\cdot}3CaSO_4{\cdot}nH_2O$). The ettringite phase formed favors the isomorphous substitution of Al^{3+} by Cr^{3+}. This was evident with the formation of calcium chromium sulfite hydrate ($Ca_4Cr_2O_6SO_3{\cdot}11H_2O$); and
3. A pozzolanic compound of calcium aluminum chromium oxide sulfate hydrate ($Ca_4Al_2Cr_{0.5}O_{10}(SO_4)_{0.5}{\cdot}16H_2O$) was also found in the samples. This compound occurs most likely as a precipitate (Dermatas and Moon 2005).

The formation of the above compounds indicates the effective immobilization of the chromium in the cement matrixes. The diffraction patterns of the 1st, 5th and 28th day old samples indicate a minor change in the intensities of the elements. The subsequent reactions between the compounds present in the sludge, and cement would have altered the intensities of the compound and setting time of the chromium/cement matrixes.

Energy dispersive X-ray diffraction analysis (EDX)/scanning electron microscope (SEM) Figure 6a–g shows the EDX/SEM analysis of the S/S matrixes. The presence of calcium, oxygen, sodium, aluminum, iron, chromium, oxygen, carbon, sulfur, chloride, silicon, etc., was observed in the S/S matrixes through EDX analysis. The analysis shows that calcium, oxygen and carbon contributed much toward the total atomic weight. Similarly, the nanoparticles and nano-biocomposites present in the sludge have significantly increased the iron content of the S/S matrixes. The SEM pictures (inset in Fig. 6a–g) represent a highly porous system, which is helpful for the entrapment of chromium ions. The C/S/ZVIN, C/S/MIN, C/S/ZVIN–SB, C/S/MIN–SB and C/FA/S/MIN–SB have shown brighter spots than C/S and C/FA/S matrixes, which may be due to the filling of pores by nanoparticles and nano-biocomposites.

Fourier transform infra-red (FTIR) spectroscopy The FTIR analysis of the S/S matrixes at 5th and 28th day of hydration is shown in the supplementary material (Figures S7; S8 and Table S4). The orthosilicate SiO_4^{4-} has a tetrahedral symmetry and four normal modes of vibrations namely v_1—symmetric stretching (811–854 cm^{-1}), v_2—in-plane bending (452 cm^{-1}), v_3—asymmetric stretching (873–997 cm^{-1}) and v_4—out-of-plane bending (513–525 cm^{-1}). The free NO_3^- ion has a planar D_{3h}

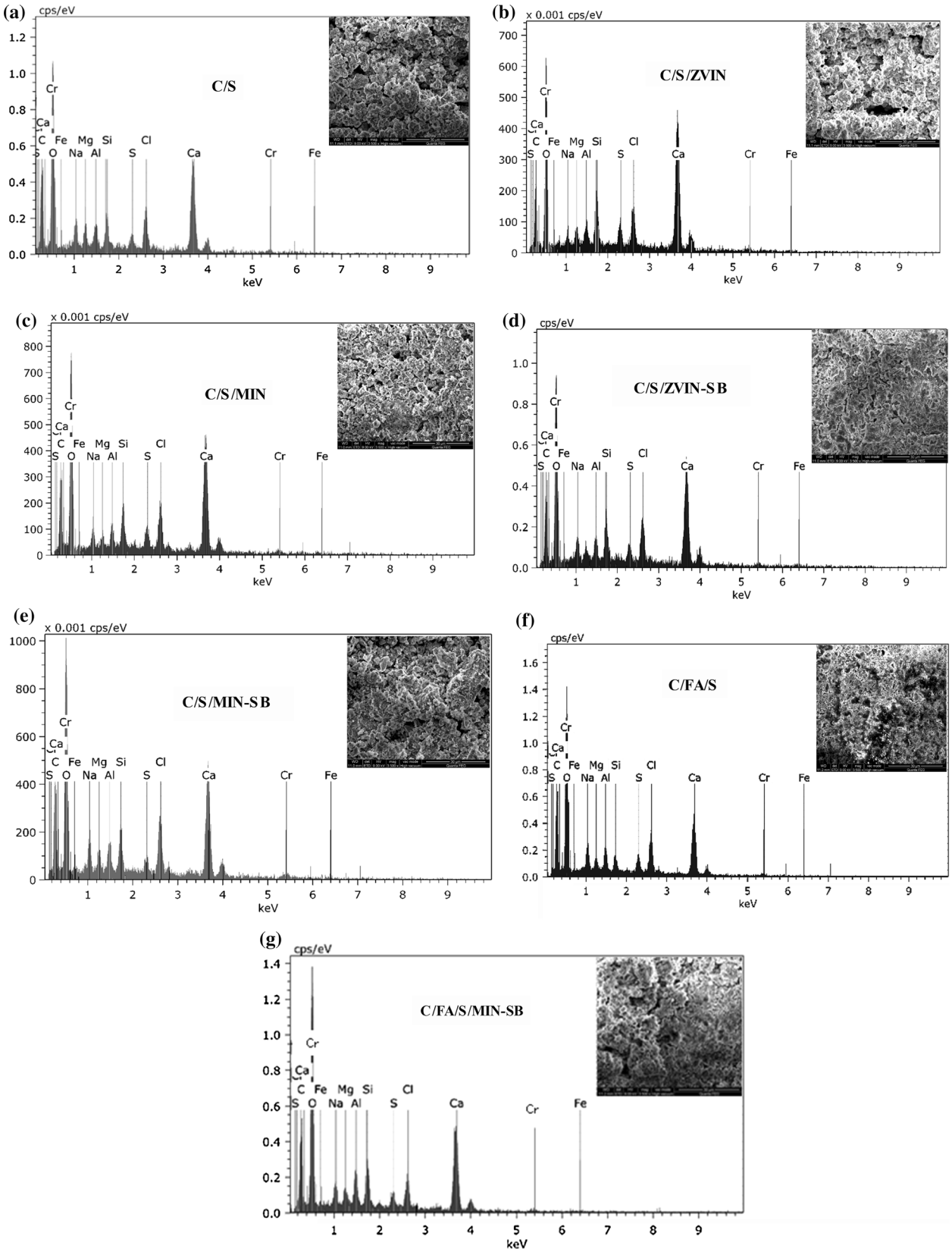

Fig. 6 EDX/SEM analysis of **a** C/S, **b** C/S/ZVIN, **c** C/S/MIN, **d** C/S/ZVIN–SB, **e** C/S/MIN–SB, **f** C/FA/S and **g** C/FA/S/MIN–SB matrixes

symmetry. NO stretching bands (v_3 and v_1) and bending vibrations (v_2 and v_4) are obtained from NO_3^- ion (Omotoso et al. 1998). The functional groups present in the S/S matrixes are indicated below.

1. The peaks between 873–997 and 513–525 cm^{-1} specify asymmetric and out-of-plane bending vibration of SiO_4^{4-} ions in the S/S matrixes.
2. The in-plane bending vibration of $SiO_4^{4-}$was also observed for all the S/S matrixes at 452 cm^{-1}.
3. The band 480.28 cm^{-1} is due to bending modes in polymeric silicate units. This band cannot be compared directly with silicate ions in the chromium doped matrixes since the band near 490 cm^{-1} overlaps with a strong Cr–O stretching vibration.
4. The broader band around 1000–1050 cm^{-1} is also due to silicon anion. This shift of peak is due to the effect of chromium in silicate tetrahedral symmetry. The degree of silicate polymerization may change because of Ca–Cr, C–S–H and chromium substituted C–S–H complexes.
5. The peaks between 1101 and 1157 cm^{-1} may be due to $v_3\,SO_4^{2-}$ (Mollah et al. 1992). The very sharp and broad peak around 1130 cm^{-1} is due to the calcium sulfate hydrate present in the S/S matrixes. The shift in the bands in this region is maybe due the presence of other sulfate compounds and the intervention of chromium ions. The other sulfate compounds present in the matrixes are sodium calcium aluminum sulfate hydrate, ettringite and calcium chromium sulfate hydrate.
6. The bands between 3300 and 3500 cm^{-1} are due to the stretching vibration of OH groups. The peaks 2500–3200, 3633.89 and 3508.52 cm^{-1} also indicate the sharp intensity peak of O–H stretching. The stretching of OH groups occurs due to hydration of the compounds present in the matrixes. The XRD analysis also confirmed the hydration process by indicating the presence of calcium hydroxide, calcium chromium hydrate, calcium aluminum oxide chromium hydrate, calcium sulfate hydrate, etc., in the S/S matrixes (Mohan 2004).
7. The peaks in the range of 1320–1450 cm^{-1} belong to the asymmetric stretch of $v_3NO_3^-$ ions. This may be due to the presence of Ca and Cr coordinating NO_3^- compounds.
8. The peak at 713.6 cm^{-1} is due to the vibrational band of $v_4\ CO_3^{2-}$ ion (Mohan 2004). This is due to the presence of calcium carbonate in the S/S matrixes.
9. The bands between 600–800, 2500–3300 and 1580–1650 cm^{-1} are due to the stretching of weak C–S groups, O–H bond from carboxylic acid and N–H in-plane bending vibration, respectively (Mohan 2004).
10. The sharp intensity peaks observed between 1535–1640 and 1770–1800 cm^{-1} indicate the stretching vibration of C=O (Mohan 2004)
11. The peaks observed between 520 and 610 cm^{-1} indicate the presence of iron oxide compounds in the S/S matrixes (Lu et al. 2010).

Thus the analysis of functional groups of the S/S matrixes shows the entrapment of chromium ions in the cement matrixes.

Conclusions

The following are the chief conclusions that can be drawn from the experimental study:

1. The S/S matrixes containing the sludge stabilized by nanoparticles and nano-biocomposites reduced the leaching rate of chromium to above 95% in comparison with the S/S matrix containing the unstabilized sludge. The cumulative fraction of chromium leached showed that the mobility of chromium ions was more in extractant 1 and less in DIW and extractant 2.
2. The dominant leaching mechanism for C/S/ZVIN, C/S/MIN, C/S/ZVIN–SB, C/S/MIN–SB and C/FA/S/MIN–SB matrixes was found to be 'diffusion,' whereas it was 'dissolution' for C/S and C/FA/S matrixes.
3. The diffusion studies indicated that chromium became immobile in all the specimens. The addition of nanoparticles and nano-biocomposites increased the values of physical retardation and chemical retention ($R\tau$) of the S/S matrixes. The mean LI was found to be higher than 13 for all the test specimens, which indicated the efficacy of S/S matrixes in controlled applications.
4. Nanoparticles and nano-biocomposites increased the compressive strength of S/S matrixes. The ZVIN, MIN, ZVIN–SB and MIN–SB increased the compressive strength of cement-based S/S matrixes by 3.7, 7.9, 7.9 and 51.7%, respectively. The C/FA/S/MIN–SB matrix showed an increase of 71.4% in compressive strength in comparison with C/FA/S matrix.
5. The instrumental analyses confirmed the binding of chromium ions in the S/S matrixes. Experimental studies indicated an insignificant leachability of chromium ions from S/S matrixes. S/S matrix containing the sludge stabilized by MIN–SB (C/S/MIN–SB) resulted in the least leachability of chromium compared to the other matrixes.

Acknowledgements The authors are thankful to the VIT University, Vellore, India, for providing facilities for carrying out this research. The first author is thankful to the CSIR, New Delhi, India, for the financial assistance provided to her as a Senior Research Fellowship (SRF).

References

Aly M, Hashmi MSJ, Olabi AG, Messeiry A, Hussain AI (2011) Effect of nanoclay particles on mechanical, thermal and physical behaviors of waste-glass cement mortars. Mater Sci Eng A 528(27):7991–7998. doi:10.1016/j.msea.2011.07.058

ANSI (1986) Measurement of the leachability of solidified low-level radioactive wastes by a short-term tests procedure. ANSI/ANS-16.1, American Nuclear Society, Illinois, USA

Arthy M, Phanikumar BR (2015) Immobilization of chromium in tannery sludge using iron-based nanoparticles and nanobiocomposites. Water Air Soil Pollut 226:1–25. doi:10.1007/s11270-015-2466-7

Arthy M, Phanikumar BR (2016) Efficacy of iron-based nanoparticles and nano-biocomposites in removal of Cr^{3+}. J Hazard Toxic Radioact Waste 20(3):1–28. doi:10.1061/(ASCE)HZ.2153-5515.0000317

ASTM (1991) Standard test method for unconfined compressive strength of cohesive soil. ASTM D2166-91, ASTM International, West Conshohocken, Pennsylvania

ASTM (2008) Standard test method for accelerated leach test for diffusive releases from solidified waste and a computer program to model diffusive, fractional leaching from cylindrical waste forms. ASTM C 1308, ASTM International, West Conshohocken, Pennsylvania. doi:10.1520/C1308-08

ASTM (2013) Standard test methods for time of setting of hydraulic cement by vicat needle. ASTM C191, ASTM International, West Conshohocken, Pennsylvania. doi:10.1520/C0191

Bulut U, Ozverdi A, Erdem M (2009) Leaching behavior of pollutants in ferrochrome arc furnace dust and its stabilization/solidification using ferrous sulphate and portland cement. J Hazard Mater 162(2–3):893–898. doi:10.1016/j.jhazmat.2008.05.114

Cao J, Zhang WX (2006) Stabilization of chromium ore processing residue (COPR) with nanoscale iron particles. J Hazard Mater 132(2–3):213–219. doi:10.1016/j.jhazmat.2005.09.008

Cullinane MJ, Jones LW (1986) Stabilization/solidification of hazardous waste, EPA/600/D-86/028, U.S. Environmental Protection Agency Hazardous Waste Engineering Laboratory (HWERL), Cincinnati, Ohio

Dermatas D, Meng X (2003) Utilization of fly ash for stabilization/solidification of heavy metal contaminated soils. Eng Geol 70(3–4):377–394. doi:10.1016/S0013-7952(03)00105-4

Dermatas D, Moon DH (2005) Chromium leaching and immobilization in treated soils. Environ Eng Sci 23(1):77–87. doi:10.1089/ees.2006.23.77

Dermatas D, Moon DH, Menounou N, Meng X, Hires R (2004) An evaluation of arsenic release from monolithic solids using a modified semi-dynamic leaching test. J Hazard Mater 116(1–2):25–38. doi:10.1016/j.jhazmat.2004.04.023

Groot GJD, Sloot HAVD (1992) Determination of leaching characteristics of waste materials leading to environmental product certification. In: Gilliam TM, Wiles CC (eds) Stabilization and solidification of hazardous radioactive and mixed wastes. ASTM STP 1123, vol 2, pp 149–170

Heimann RB, Conrad D, Florence LZ, Neuwirth M, Ivey DG, Mikula RJ, Lam WW (1992) Leaching of simulated heavy metal waste stabilized/solidified in different cement matrixes. J Hazard Mater 31(1):39–57. doi:10.1016/0304-3894(92)87038-H

Kanchinadham SBK, Narasimman LM, Pedaballe V, Kalyanaraman C (2015) Diffusion and leachability index studies on stabilization of chromium contaminated soil using fly ash. J Hazard Mater 297:52–58. doi:10.1016/j.jhazmat.2015.04.045

Kumpiene J, Lagerkvist A, Maurice C (2008) Stabilization of As, Cr, Cu, Pb and Zn in soil using amendments: a review. Waste Manag 28(1):215–225. doi:10.1016/j.wasman.2006.12.012

Kundu S, Gupta AK (2008) Immobilization and leaching characteristics of arsenic from cement and/or lime solidified/stabilized spent adsorbent containing arsenic. J Hazard Mater 153(1–2):434–443. doi:10.1016/j.jhazmat.2007.08.073

Lea FM (1971) The chemistry of cement and concrete, 3rd edn. Chemical Publishing Company, New York

Lee D (2004) Leachability of Pb-doped solidified waste forms using Portland cement and calcite: III. Insight of leaching mechanism. Environ Eng Res 9(4):175–183. doi:10.4491/eer.2004.9.4.175

Li YH, Gregory S (1974) Diffusion of ions in sea water and in deep-sea sediments. Geochim Cosmochim Acta 38(5):703–714. doi:10.1016/0016-7037(74)90145-8

Li XQ, Cao J, Zhang WX (2008) Stoichiometry of Cr(VI) immobilization using nanoscale zero-valent iron (nZVI): a study with high resolution X-ray photoelectron spectroscopy (HR-XPS). Ind Eng Chem Res 47(7):2131–2139. doi:10.1021/ie061655x

Lu W, Shen Y, Xie A, Zhang W (2010) Green synthesis and characterization of superparamagnetic Fe_3O_4 nanoparticles. J Mag Mag Mater 322(13):1828–1833. doi:10.1016/j.jmmm.2009.12.035

Malviya R, Chaudhary R (2006) Factors affecting hazardous waste solidification/stabilization: a review. J Hazard Mater 137(1):267–276. doi:10.1016/j.jhazmat.2006.01.065

Mattigod SV, Lindberg MJ, Westsik JH, Parker KE, Chung CW (2011) Waste acceptance testing of secondary waste forms: cast Stone, Ceramicrete and DuraLith. PNNL report 20632, Richland, Washington

Mohan J (2004) Organic spectroscopy principles and applications, 2nd edn. Narosa Publishing House, New Delhi

Mollah MYA, Tsai YN, Hess TR, Cocke DL (1992) An FTIR, SEM and EDS investigation of solidification/stabilization of chromium using Portland cement type V and type IP. J Hazard Mater 30(3):273–283. doi:10.1016/0304-3894(92)87004-Y

Nathwani JS, Phillips CR (1980) Leachability of Ra-226 from uranium mill tailings consolidated with naturally occurring materials and/or cement: analysis based on mass transport equation. Water Air Soil Poll 14(1):389–402. doi:10.1007/BF00291851

Omotoso OE, Ivey DG, Mikula R (1995) Characterization of chromium doped tricalcium silicate using SEM/EDS, XRD and FTIR. J Hazard Mater 42(1):87–102. doi:10.1016/0304-3894(95)00012-J

Omotoso OE, Ivey DG, Mikula R (1998) Containment mechanism of trivalent chromium in tricalcium silicate. J Hazard Mater 60(1):1–28. doi:10.1016/0304-3894(95)00012-J

Park JY, Batchelor B (1999a) Prediction of chemical speciation in stabilized/solidified wastes using a general chemical equilibrium model II: doped waste contaminants in porewaters. Cem Concr Res 29(1):99–105. doi:10.1016/S0008-8846(98)00181-1

Park JY, Batchelor B (1999b) Prediction of chemical speciation in stabilized/solidified wastes using a general chemical equilibrium model Part I. Chemical representation of cementitious binders. Cem Concr Res 29(3):361–368. doi:10.1016/S0008-8846(98)00218-X

Phenrat T, Marhaba TF, Rachakornkij M (2005) A SEM and X-ray study for investigation of solidified/stabilized arsenic–iron hydroxide sludge. J Hazard Mater 118(1–3):185–195. doi:10.1016/j.jhazmat.2004.10.019

Powell RM, Puls RW, Hightower SK, Sabatini DA (1995) Coupled iron corrosion and chromate reduction: mechanisms for subsurface remediation. Environ Sci Technol 29(8):1913–1922. doi:10.1021/es00008a008

Radovanovic DD, Kamberovic ZJ, Korac MS, Rogan JR (2016) Solidified structure and leaching properties of metallurgical wastewater treatment sludge after solidification/stabilization process. J Environ Sci Health A Toxic Hazard Subst Environ Eng 51(1):34–43. doi:10.1080/10934529.2015.1079104

Rossetti VA, Medici F (1996) Inertization of toxic metals in cement matrixes: effect on hydration, setting and hardening. Cem Concr Res 25(6):1147–1152. doi:10.1016/0008-8846(95)00106-M

Shi C, Spence R (2004) Designing of cement-based formula for solidification/stabilization of hazardous, radioactive and mixed wastes. Crit Rev Environ Sci Technol 34(4):391–417. doi:10.1080/10643380490443281

Shu J, Liu R, Liu Z, Chen H, Du J, Tao C (2016) Solidification/stabilization of electrolytic manganese residue using phosphate resource and low-grade MgO/CaO. J Hazard Mater 317:267–274. doi:10.1016/j.jhazmat.2016.05.076

Singh R, Misra V, Singh RP (2011) Synthesis, characterization and role of zero-valent iron nanoparticle in removal of hexavalent chromium from chromium-spiked soil. J Nanopart Res 13(9):4063–4073. doi:10.1007/s11051-011-0350-y

Singh R, Misra V, Singh RP (2012) Removal of hexavalent chromium from contaminated ground water using zero-valent iron nanoparticles. Environ Monit Assess 184(6):3643–3651. doi:10.1007/s10661-011-2213-5

Sloot HAVD, Groot GJD, Wijkstra J (1989) Leaching characteristics of construction materials and stabilization products containing waste materials. In: Cote PL, Gilliam TM (eds) Environmental aspects of stabilization and solidification of hazardous and radioactive wastes. ASTM STP 1033, Philadelphia, pp 125–149. doi:10.1520/STP22875S

Swarnalatha S, Ramani K, Karthi AG, Sekaran G (2006) Starved air combustion solidification/stabilization of primary chemical sludge from a tannery. J Hazard Mater 137(1):304–313. doi:10.1016/j.jhazmat.2006.02.006

Taylor HFW (1990) Cement chemistry. Academic Press, London

Torras J, Buj I, Rovira M, Pablo JD (2011) Semi-dynamic leaching tests of nickel containing wastes stabilized/solidified with magnesium potassium phosphate cements. J Hazard Mater 186(2–3):1954–1960. doi:10.1016/j.jhazmat.2010.12.093

Valls S, Vazquez E (2002) Leaching properties of stabilized/solidified cement-admixtures-sewage sludges systems. Waste Manag 22(1):37–45. doi:10.1016/S0956-053X(01)00027-7

Wang S, Vipulanandan C (2000) Solidification/stabilization of Cr(VI) with cement leachability and XRD analyses. Cem Concr Res 30(3):385–389. doi:10.1016/S0008-8846(99)00265-3

Wang T, Jin X, Chen Z, Megharaj M, Naidu R (2014a) Simultaneous removal of Pb(II) and Cr(III) by magnetite nanoparticles using various synthesis conditions. J Ind Eng Chem 20(5):3543–3549. doi:10.1016/j.jiec.2013.12.047

Wang Y, Fang Z, Liang B, Tsang EP (2014b) Remediation of hexavalent chromium contaminated soil by stabilized nanoscale zero-valent iron prepared from steel pickling waste liquor. Chem Eng J 247:283–290. doi:10.1016/j.cej.2014.03.011

Wastewater Technology Centre (1991) Proposed evaluation protocol for cement based solidified wastes. Environment Canada report EPS 3/HA/9, Ottawa, Ontario, Canada

Yousuf M, Mollah A, Vempati RK, Lin TC, Cocke DL (1995) The interfacial chemistry of solidification/stabilization of metals in cement and pozzolanic material systems. Waste Manag 15(2):137–148. doi:10.1016/0956-053X(95)00013-P

Zha X, Wang H, Xie P, Wang C, Dangla P, Ye J (2016) Leaching resistance of hazardous waste cement solidification after accelerated carbonation. Cem Concr Compos 72:125–132. doi:10.1016/j.cemconcomp.2016.06.001